crystals

MDPI

Article

Interlayer Coupling and Pressure Engineering in Bilayer MoS_2

Wei Qiao [1,2], Hao Sun [1,2], Xiaoyue Fan [1,2], Meiling Jin [3], Haiyang Liu [1,2], Tianhong Tang [1,2], Lei Xiong [1,2], Binghui Niu [1,2,*], Xiang Li [1,2] and Gang Wang [1,2,*]

1 Centre for Quantum Physics, Key Laboratory of Advanced Optoelectronic Quantum Architecture and Measurement (MOE), School of Physics, Beijing Institute of Technology, Beijing 100081, China; qiaowei@bit.edu.cn (W.Q.); haosun@bit.edu.cn (H.S.); fanxy@bit.edu.cn (X.F.); liuhaiyang21@bit.edu.cn (H.L.); tangth@bit.edu.cn (T.T.); 3120191463@bit.edu.cn (L.X.); xiangli@bit.edu.cn (X.L.)

2 Beijing Key Laboratory of Nanophotonics & Ultrafine Optoelectronic Systems, Beijing Institute of Technology, Beijing 100081, China

3 Department of Physics, Southern University of Science and Technology, Shenzhen 518055, China; jinml@sustech.edu.cn

* Correspondence: binghui.niu@bit.edu.cn (B.N.); gw@bit.edu.cn (G.W.)

Abstract: Controlling the interlayer coupling by tuning lattice parameters through pressure engineering is an important route for tailoring the optoelectronic properties of two-dimensional materials. In this work, we report a pressure-dependent study on the exciton transitions of bilayer MoS_2 exfoliated on a diamond anvil surface. The applied hydrostatic pressure changes from ambient pressure up to 11.05 GPa using a diamond anvil cell device. Raman, photoluminescence, and reflectivity spectra at room temperature are analyzed to characterize the interlayer coupling of this bilayer system. With the increase of pressure, the indirect exciton emission disappears completely at about 5 GPa. Importantly, we clearly observed the interlayer exciton from the reflectivity spectra, which becomes invisible at a low pressure around 1.26 GPa. This indicates that the interlayer exciton is very sensitive to the hydrostatic pressure due to the oscillator strength transfer from the direct transition to the indirect one.

Keywords: 2D materials; interlayer coupling; bilayer MoS_2; pressure engineering

check for updates

Citation: Qiao, W.; Sun, H.; Fan, X.; Jin, M.; Liu, H.; Tang, T.; Xiong, L.; Niu, B.; Li, X.; Wang, G. Interlayer Coupling and Pressure Engineering in Bilayer MoS_2. *Crystals* **2022**, *12*, 693. https://doi.org/10.3390/cryst12050693

Academic Editor: Giancarlo Salviati

Received: 24 April 2022
Accepted: 11 May 2022
Published: 12 May 2022

Publisher's Note: MDPI stays neutral with regard to jurisdictional claims in published maps and institutional affiliations.

Copyright: © 2022 by the authors. Licensee MDPI, Basel, Switzerland. This article is an open access article distributed under the terms and conditions of the Creative Commons Attribution (CC BY) license (https://creativecommons.org/licenses/by/4.0/).

1. Introduction

Van der Waals (vdW) materials have attracted considerable attention due to their fascinating physical properties. Semiconducting transition metal dichalcogenides (TMDCs), MX_2 (where M is a transition metal of group VI (Mo, W) and X is a chalcogen (S, Se), such as MoS_2, WS_2, WSe_2, and $MoSe_2$) exhibit an indirect-to-direct band gap transition as the thickness decreases to a monolayer. The light-matter interaction in monolayer TMDCs is dominated by the excitonic effects, enabling many possible applications in photonic and optoelectronic techniques within the visible and near infrared range [1–5]. Due to the weak interlayer interaction, the stacking of vdW materials becomes an important way to intrude exotic properties without considering the crystal mismatch. The various interlayer excitons in TMDC heterostructures show huge advantages in novel many-body physics, optical communication and signal processing at the on-chip level [6]. However, the weak vdW interaction also means the inefficient interlayer coupling, which hinders the comprehensive control of the layered structures. The hydrostatic pressure generated by a diamond anvil cell (DAC) has been used as an effective strategy to tune the lattice constant and the interlayer distance. The changes of electronic structure and phase transition of TMDCs mono- or thin layers using pressure control have been evidenced [7]. Similarly, the interlayer excitons in TMDCs heterobilayers have been explored under pressures [8,9], which further confirms pressure engineering as an efficient tuning tool of the two-dimensional (2D) vdW stacks.

Here in this work, we focus on the MoS_2, the representative TMDC that has attracted extensive research interests [1]. Monolayer MoS_2 is composed of a single layer of the

transition metal molybdenum (Mo) and two layers of chalcogen (S) and thus forms what is known as a MoS_2 sandwiched structure. The structures of few-layer and bulk MoS_2 are constituted by naturally 2H stacking MoS_2 monolayers by the weak vdW interaction. In the monolayer limit, the clear optical resonances from direct K–K transition provide crucial benchmark for the real 2D excitons. The excitons in 2D semiconductors possess relatively large binding energy and in-plane optical transition dipole. In the 2H homobilayer TMDCs system such as MoS_2 and $MoSe_2$, the interlayer excitons were evidenced as well [10,11]. This type of indirect exciton has larger oscillator strength than the usual interlayer exciton in heterobilayer systems [12,13]. In bilayer MoS_2, due to the interlayer exciton degeneracy and the out-of-plane dipole nature, the wide energy tuning of the transition ranges up to 120 meV and exciton-exciton interactions were unveiled [14].

To date, only a few studies have been focusing on bilayer MoS_2 under high pressure, especially considering the interlayer exciton. In this work, we provide systematic optical measurements of bilayer MoS_2 under hydrostatic pressure. The different behaviors of monolayer and bilayer MoS_2 are analyzed. The pressure-dependent measurements of the Raman, photoluminescence (PL), and reflectivity spectra up to 11.05 GPa are analyzed to explore the interlayer coupling and the interlayer exciton. With the increasing of pressure, the A and B exciton splitting of 2H bilayer MoS_2 becomes larger as the enhanced interlayer coupling at smaller interlayer distance. The indirect exciton emission is quenched completely at about 5 GPa. Importantly, we clearly resolve the interlayer exciton from the reflectivity spectra of the bilayer MoS_2 sample, which becomes invisible quickly at a low pressure around 1.26 GPa. This indicates that the interlayer exciton is very sensitive to the hydrostatic pressure due to the transition of the band structure.

2. Experimental Method

Hydrostatic pressure on MoS_2 samples was applied by a symmetric diamond anvil cell (DAC) that consists of two opposing anvils sitting on supporting plates. Diamond anvils with culet diameters of 300 μm were used for this study. T301 stainless steel and BeCu gaskets were pre-indented and then drilled with a hole of 150 μm in diameter. Mineral oil and silicone oil were used as pressure transmission medium (PTM). The wavelength shift of ruby fluorescence was used to measure the pressure in the DAC [15]. The schematic diagram is shown in Figure 1a.

The investigated MoS_2 flakes, including monolayer, bilayer, and bulk MoS_2, were fabricated by the mechanical exfoliation with adhesive tape from a bulk crystal (2D semiconductors, Inc., Scottsdale, AZ, USA). Then the MoS_2 samples were transferred onto a diamond anvil surface, which also served as the substrate in the sample chamber, with the help of polydimethylsiloxane (PDMS). The typical optical images of monolayer and few-layer MoS_2 are firstly identified by optical contrast under a microscope, as depicted in Figure 1b. Optical images indicate that the samples are successfully transferred to the DAC chamber, and the Raman and PL spectral measurements under ambient conditions furthermore confirm the successful sample loading. No noticeable folding or bending was observed in the MoS_2 samples during pressurization.

Both the Raman and PL were measured with a 532 nm CW laser excitation, while the reflectance spectra were measured with a broadband tungsten-halogen lamp. The signal from the samples were collected through spectrometer with a liquid nitrogen-cooled charge-coupled device detector, and all measurements were performed at room temperature. All spectra were collected in a backscattering geometry using 1200 g/mm or 300 g/mm grating. To avoid the damage of samples by heating or by radiation, the laser power was set to the order of microwatts.

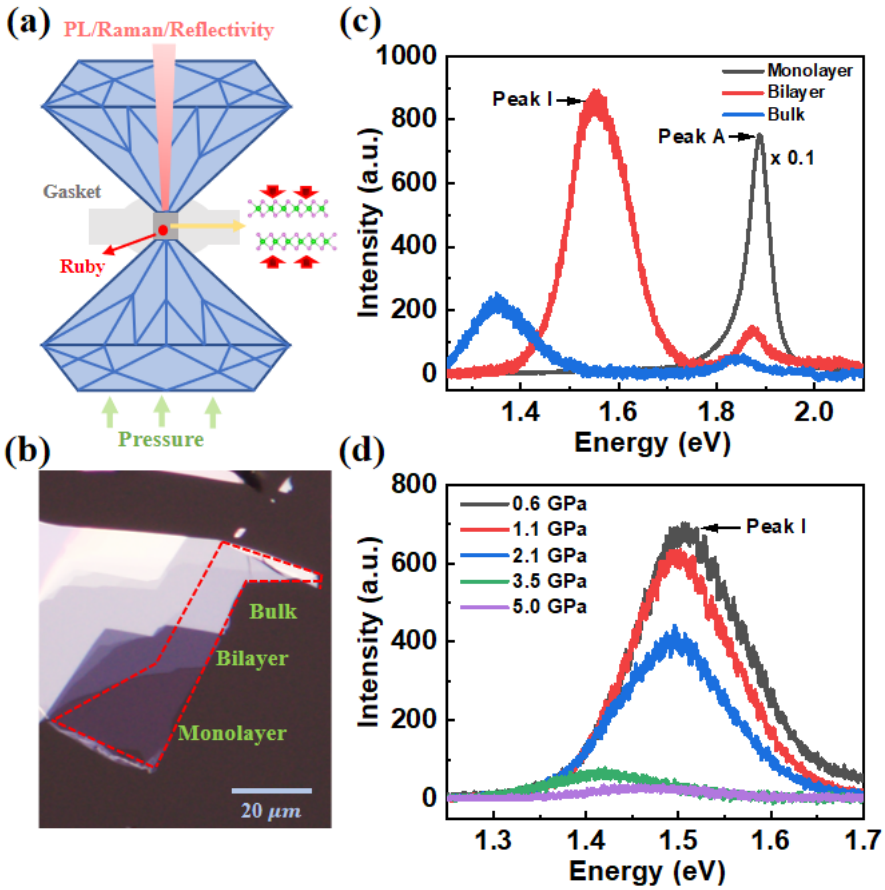

Figure 1. (**a**) Schematic diagram of DAC, which is mainly composed of atop anvil, bottom anvil and gasket. (**b**) Optical microscope images of monolayer, bilayer and bulk MoS_2 on top of PDMS. (**c**) PL spectra of monolayer, bilayer, and bulk MoS_2 without the top anvil. (**d**) PL spectra of bilayer MoS_2 at different pressures.

3. Results and Discussion

The PL spectra of the monolayer, bilayer and bulk of MoS_2 under ambient conditions are shown in Figure 1c. For monolayer and bilayer MoS_2, the PL peak labeled A at ~1.886 and 1.875 eV, respectively, is assigned to a direct K-K exciton transition between the conduction band (CB) and the upper lying valence band (VB). For the bilayer and bulk, the indirect transition between the K-valley of the CB and the Γ point of the VB are located at ~1.561 and 1.358 eV. The emissions from the bulk MoS_2 were reported absent initially in the seminal work [3]. The similar PL of bulk to our result were evidenced as well by different groups [16,17]. This may arise from the various sample source or the different actual thickness of the flakes, which requires further studies. As the number of layers increased, the PL peak I shifts to a lower energy position, while the energies of the A excitons related to the K–K interband transition undergo no clear shift. It is known that the CB valley and the VB extrema at the K point are primarily constituted by d orbital wave functions that are localized around the Mo atoms [3]. They therefore possess weak interlayer coupling as the Mo atoms are in the middle of the sandwich structure. By contrast, the valence top at the Γ point is described by the wave function of S atoms and extends beyond the plane of MoS_2 structure. Thus, the indirect transitions show obvious tuning through the interlayer distance due to the strong interlayer coupling.

The indirect exciton PL spectra of bilayer MoS_2 with increasing pressures are shown in Figure 1d. The direct A exciton emissions are not shown as the overlap with PTM background signals. Here, the periodic oscillation is caused by the interference between the upper and lower anvil surfaces of the diamond. We noted that the energy shift of peak I between 1 atm and 0.6 GPa is relatively large, which is due to the combined effect

of both pressure and dielectric environment changes. The enhanced dielectric constant in the chamber of DAC will decrease both the quasiparticle and binding energy of the exciton. This could lead to a further redshift of the indirect exciton emission I apart from the pressure-induced one. With the increase of pressure (ambient to 3.5 GPa), Peak I of bilayer MoS_2 shows a clear redshift and decreasing of intensity. At 2.1 GPa, the clear hump around 1.43 eV is resolved in our measurements. This is due to the coexistence of Γ–Λ and Γ–K contributes to the indirect peak I. However, these two components should have different sensitivities to the pressure. Thus, the explicit assignments of the individual transitions require further precise calculations. This broadening and double-peak spectral feature confirm the K–Λ crossover in the conduction band. The transition energy shifts more than 100 meV and the intensity disappears at around 5 GPa, which is similar to the results reported by Dou et al. [18] The decrease in the Γ–K gap with pressure suggests that the VB and CB move closer via compression, due to the large band splitting at Γ that originated from interlayer electronic coupling [19]. It is noteworthy that the turning point is observed at ~5 GPa, where an electronic structure phase transition may occur [20]. At that point, the conduction band minimum in the Brillouin zone may change to Λ from K point. This process starts around 2 GPa and thus the peak I has component Γ–Λ transition with different pressure sensitivity compared to the Γ–K energy gap. Most likely this is the reason for the different shift rates in the 0.6–2.1 GPa and 2.1–3.5 GPa.

In order to further understand the pressure effect on the lattice vibrations of MoS_2, we analyzed the Raman spectra of MoS_2 at different pressures. Figure 2a–c depict the pressure-dependent Raman spectra of the monolayer, bilayer, and bulk MoS_2 at room temperature. It can be seen that with increasing pressure, the Raman spectrum retains a two-peak shape up to 10.37 GPa. Both the A_{1g} and E^1_{2g} modes shift to higher energy due to the strengthening of intra-atom interactions under hydrostatic pressure. The shift rate of all Raman modes for monolayer, bilayer and bulk with pressure are shown in Figure 2d–f, respectively. We note that the blue-shift rate of A_{1g} mode is higher than that of E^1_{2g} mode for all of them with the increasing energy difference between the two modes, which suggests that the transverse movement of S–S bonds is more significantly affected than the in-plane bonds during compression [20,21].

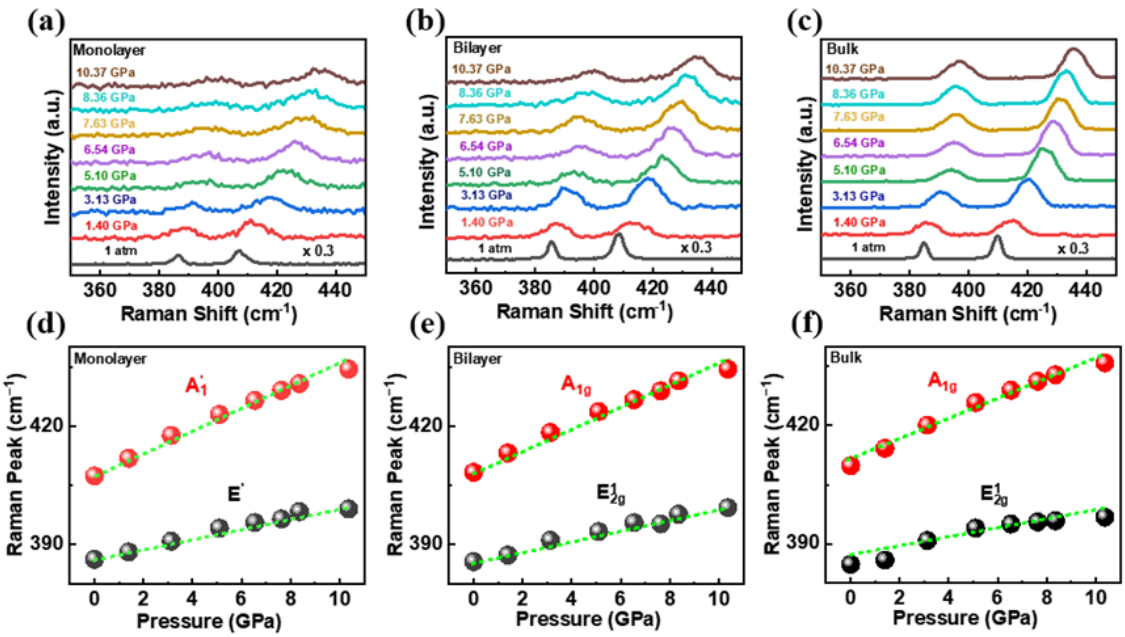

Figure 2. Raman spectra of (**a**) monolayer, (**b**) bilayer, and (**c**) bulk MoS_2 at different pressures. (**d**–**f**) Raman peaks of monolayer, bilayer and bulk MoS_2 as a function of pressure.

The reflectance spectra of the monolayer and bilayer MoS_2 were measured without the top diamond anvil, as displayed in Figure 3a. The reflectance is calculated as $\Delta R/R = (R_{sam} - R_{sub})/R_{sam}$, where R_{sam} is the intensity reflection coefficient of the sample and R_{sub} is for the substrate. Three absorption peaks corresponding to the A, B, and C excitons are clearly resolved. For monolayer MoS_2, the energy position of peak A at 1.902 eV exhibit a small blueshift to the exciton emission peak in the PL spectra. Here, the value of blueshift may be related to the difference in excitation power and Stokes shift. For the bilayer sample, the A and B exciton energy splitting is around 176 meV. Both A and B excitons are formed by the states at the K point, where the spin-orbit splittings are around a few meV and 150 meV in CB and VB, respectively. The energy difference between peaks of A and B in the monolayer limit is dominated by the spin-orbit coupling in the VB with modifications from the binding energy and exchange term [22]. In bilayer MoS_2, being 2H stacking in our case, the larger A–B splitting is due to the interlayer coupling.

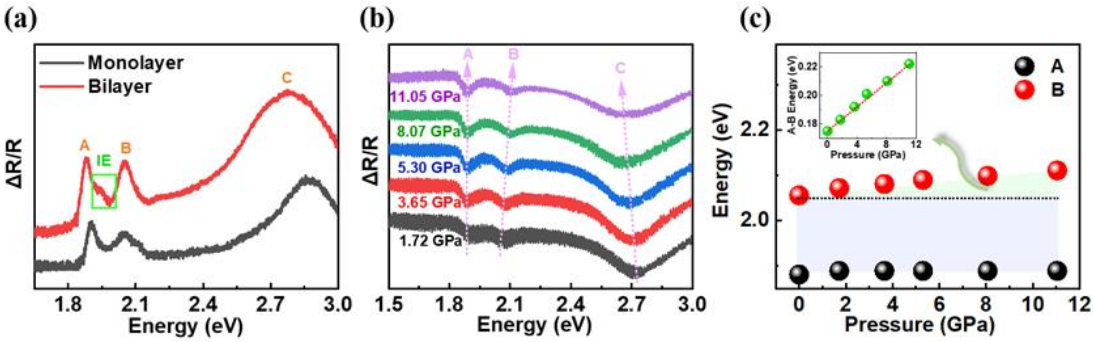

Figure 3. (**a**) The reflectivity spectra of monolayer and bilayer MoS_2 without the top diamond anvil (under ambient conditions); A, B and C are the exciton transitions. (**b**) Pressure-dependent reflectivity spectra of bilayer MoS_2. (**c**) Dependence of A and B energy on the pressure for bilayer MoS_2. Inset: the energy splitting between A and B exciton as a function of pressure.

Figure 3b shows the pressure-dependent reflectivity spectra of bilayer MoS_2. The reversed reflectivity signal is due to the change of the refractive index combination between the medium above and below of the sample after the DAC was sealed with the PTM and the second diamond. It can be seen that with the increasing pressure, the A exciton is almost unchanged while B is gradually blue-shifted. The splitting energy between A and B excitons increases nearly linearly from 176 meV under ambient pressure to 222 meV at the pressure of 11.05 GPa (see Figure 3c inset). The pressure-induced enhancement of the splitting arises from the larger interlayer hopping term at smaller interlayer spacing. In addition, the C exciton shows a slight redshift as the pressure increases from 1.72 to 11.05 GPa.

More importantly, prominent interlayer exciton (IE) is visible between the A and B excitons at 1.944 eV (i.e., 64 meV above the A exciton in bilayer MoS_2 under ambient pressure (Figure 4a)). This feature is in good agreement with the very recent results in high quality and hBN encapsulated 2H MoS_2 bilayers [10,23,24]. The interlayer exciton also forms at the K point with electron in one layer but the hole delocalized over the two. Previous GW + BSE calculations and reflectivity measurements at 4 K unveiled the unique nature of this transition: the valence band maximum hole state in one layer partially hybridized with the lower hole state in the second layer and the electron is well-localized in the second layer as well [10]. This type of interlayer exciton combines both high oscillator strength and large out-of-plane static dipole moment [13]. With the pressure increased, the IE transition shows a relative constant transition energy but the oscillator strength decreases gradually as depicted in Figure 4b. As for the interlayer distance decreases, more significant interlayer coupling are expected, which is indeed demonstrated in Figure 3c. However, the absorption of interlayer exciton is determined by the band structures as well. When the pressure increases, the K–K transition is no longer the lowest-energy one and most of

transition strength transfers to the one from VB Γ or K point to CB Λ point [18,20]. Under higher hydrostatic pressure, the competition between these two mechanisms determines the IE response. In our measurements, the IE absorption disappears at around 1.26 GPa, which suggests the band structure transition plays a key role at higher pressure.

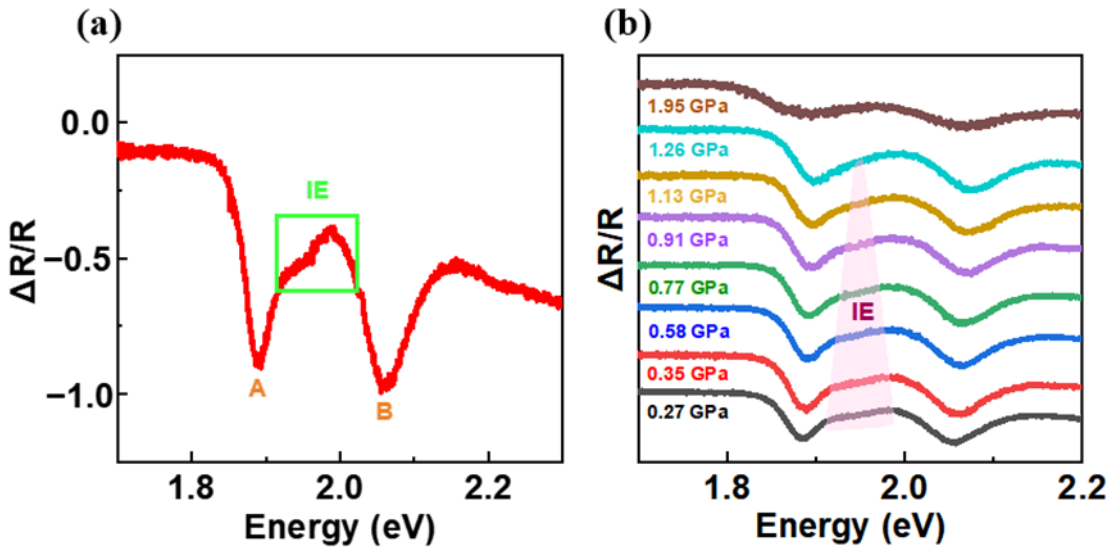

Figure 4. (**a**) The reflectivity spectrum of bilayer MoS_2 under ambient pressure. (**b**) Pressure-dependent reflectivity spectra of bilayer.

4. Conclusions

In this work, we have investigated the Raman, PL, and reflectivity spectra of monolayer, bilayer, and bulk MoS_2 under different pressures. The indirect peak of bilayer MoS_2 shows a redshift with increasing pressure and quenches at around 5 GPa. The interlayer exciton with large oscillator strength is clearly resolved in reflectivity, which is due to the interlayer coupling in 2H stacking. At higher pressures, the A–B splitting increase linearly but the IE response disappears at around 1.26 GPa. Our results suggests that the IE transition is sensitive to the interlayer distance tuning as band transformation dominates at relative low pressure. The unique optical behaviors and the interlayer nature of IE in 2H bilayer MoS_2 provide a crucial strategy for the applications using strongly coupled exciton or polaritons towards novel quantum techniques.

Author Contributions: Conceptualization, B.N., X.L. and G.W.; methodology, W.Q., H.S., X.F. and M.J.; validation, H.L., T.T. and L.X.; formal analysis, W.Q. and B.N.; investigation, W.Q.; resources, M.J., X.L. and G.W.; data curation, W.Q. and B.N.; writing—original draft preparation, W.Q. and B.N.; writing—review and editing, B.N., X.L. and G.W.; visualization, W.Q. All authors have read and agreed to the published version of the manuscript.

Funding: This research was funded by the National Natural Science Foundation of China (Grants No. 11904019, 12074033, 12004161, 11904020, 12174025), the Beijing Natural Science Foundation (Grant No. Z190006).

Institutional Review Board Statement: Not applicable.

Informed Consent Statement: Not applicable.

Data Availability Statement: The data presented in this study are available on request from the corresponding author.

Conflicts of Interest: The authors declare no conflict of interest.

References

1. Mak, K.F.; Lee, C.; Hone, J.; Shan, J.; Heinz, T.F. Atomically thin MoS_2: A new direct-gap semiconductor. *Phys. Rev. Lett.* **2010**, *105*, 136805. [CrossRef] [PubMed]
2. Radisavljevic, B.; Radenovic, A.; Brivio, J.; Giacometti, V.; Kis, A. Single-layer MoS_2 transistors. *Nat. Nanotechnol.* **2011**, *6*, 147–150. [CrossRef] [PubMed]
3. Splendiani, A.; Sun, L.; Zhang, Y.B.; Li, T.S.; Kim, J.; Chim, C.Y.; Galli, G.; Wang, F. Emerging photoluminescence in monolayer MoS_2. *Nano Lett.* **2010**, *10*, 1271–1275. [CrossRef] [PubMed]
4. Lopez-Sanchez, O.; Lembke, D.; Kayci, M.; Radenovic, A.; Kis, A. Ultrasensitive photodetectors based on monolayer MoS_2. *Nat. Nanotechnol.* **2013**, *8*, 497–501. [CrossRef]
5. Zeng, H.L.; Dai, J.F.; Yao, W.; Xiao, D.; Cui, X.D. Valley polarization in MoS_2 monolayers by optical pumping. *Nat. Nanotechnol.* **2012**, *7*, 490–493. [CrossRef]
6. Jiang, Y.; Chen, S.; Zheng, W.; Zheng, B.; Pan, A. Interlayer exciton formation, relaxation, and transport in TMD van der Waals heterostructures. *Light Sci. Appl.* **2021**, *10*, 1–29. [CrossRef]
7. Fu, L.; Wan, Y.; Tang, N.; Ding, Y.; Gao, J.; Yu, J.; Guan, H.; Zhang, K.; Wang, W.; Zhang, C.; et al. K-Λ crossover transition in the conduction band of monolayer MoS_2 under hydrostatic pressure. *Sci. Adv.* **2017**, *3*, e1700162. [CrossRef]
8. Ma, X.; Fu, S.; Ding, J.; Liu, M.; Bian, A.; Hong, F.; Sun, J.; Zhang, X.; Yu, X.; He, D. Robust Interlayer Exciton in $WS_2/MoSe_2$ van der Waals Heterostructure under High Pressure. *Nano Lett.* **2021**, *21*, 8035–8042. [CrossRef]
9. Xia, J.; Yan, J.X.; Wang, Z.H.; He, Y.M.; Gong, Y.J.; Chen, W.Q.; Sum, T.C.; Liu, Z.; Ajayan, P.M.; Shen, Z.X. Strong coupling and pressure engineering in WSe_2–$MoSe_2$ heterobilayers. *Nat. Phys.* **2021**, *17*, 92–98. [CrossRef]
10. Gerber, I.C.; Courtade, E.; Shree, S.; Robert, C.; Taniguchi, T.; Watanabe, K.; Balocchi, A.; Renucci, P.; Lagarde, D.; Marie, X.; et al. Interlayer excitons in bilayer MoS_2 with strong oscillator strength up to room temperature. *Phys. Rev. B* **2019**, *99*, 035443. [CrossRef]
11. Horng, J.; Stroucken, T.; Zhang, L.; Paik, E.Y.; Deng, H.; Koch, S.W. Observation of interlayer excitons in $MoSe_2$ single crystals. *Phys. Rev. B* **2018**, *97*, 241404. [CrossRef]
12. Paradisanos, I.; Shree, S.; George, A.; Leisgang, N.; Robert, C.; Watanabe, K.; Taniguchi, T.; Warburton, R.J.; Turchanin, A.; Marie, X.; et al. Controlling interlayer excitons in MoS_2 layers grown by chemical vapor deposition. *Nat. Commun.* **2020**, *11*, 1–7. [CrossRef]
13. Zhang, C.; Chuu, C.; Ren, X.; Li, M.; Li, L.; Jin, C.; Chou, M.; Shih, C. Interlayer couplings, Moiré patterns, and 2D electronic superlattices in MoS_2/WSe_2 hetero-bilayers. *Sci. Adv.* **2017**, *3*, e1601459. [CrossRef]
14. Leisgang, N.; Shree, S.; Paradisanos, I.; Sponfeldner, L.; Robert, C.; Lagarde, D.; Balocchi, A.; Watanabe, K.; Taniguchi, T.; Marie, X.; et al. Giant Stark splitting of an exciton in bilayer MoS_2. *Nat. Nanotechnol.* **2020**, *15*, 901–907. [CrossRef]
15. Mao, H.K.; Xu, J.; Bell, P.M. Calibration of the ruby pressure gauge to 800 kbar under quasi-hydrostatic conditions. *J. Geophys. Res.* **1986**, *91*, 4673. [CrossRef]
16. Placidi, M.; Dimitrievska, M.; Izquierdo-Roca, V.; Fontané, X.; Castellanos-Gomez, A.; Pérez-Tomás, A.; Mestres, N.; Espindola-Rodriguez, M.; López-Marino, S.; Neuschitzer, M.; et al. Multiwavelength excitation Raman scattering analysis of bulk and two-dimensional MoS_2: Vibrational properties of atomically thin MoS_2 layers. *2D Mater.* **2015**, *2*, 035006. [CrossRef]
17. Yang, L.; Cui, X.; Zhang, J.; Wang, K.; Shen, M.; Zeng, S.; Shadi, A.; Dayeh, S.; Feng, L.; Xiang, B. Lattice strain effects on the optical properties of MoS_2 nanosheets. *Sci. Rep.* **2014**, *4*, 1–7. [CrossRef]
18. Dou, X.; Ding, K.; Jiang, D.; Sun, B. Tuning and identification of interband transitions in monolayer and bilayer molybdenum disulfide using hydrostatic pressure. *ACS Nano* **2014**, *8*, 7458–7464. [CrossRef]
19. Fan, X.; Chang, C.-H.; Zheng, W.; Kuo, J.-L.; Singh, D.J. The electronic properties of single-layer and multilayer MoS_2 under high pressure. *J. Phys. Chem. C* **2015**, *119*, 10189–10196. [CrossRef]
20. Li, C.; Liu, Y.; Yang, Q.; Zheng, Q.; Yan, Z.; Han, J.; Lin, J.; Wang, S.; Qi, J.; Liu, Y.; et al. Tuning of Optical Behavior in Monolayer and Bilayer Molybdenum Disulfide Using Hydrostatic Pressure. *J. Phys. Chem. Lett.* **2021**, *13*, 161–167. [CrossRef]
21. Cheng, X.; Li, Y.; Shang, J.; Cheng, X.; Li, Y.; Shang, J.; Hu, C.; Ren, Y.; Liu, M.; Qi, Z. Thickness-dependent phase transition and optical behavior of MoS_2 films under high pressure. *Nano Res.* **2018**, *11*, 855–863. [CrossRef]
22. Robert, C.; Han, B.; Kapuscinski, P.; Delhomme, A.; Faugeras, C.; Amand, T.; Molas, M.R.; Bartos, M.; Watanabe, K.; Taniguchi, T.; et al. Measurement of the spin-forbidden dark excitons in MoS_2 and $MoSe_2$ monolayers. *Nat. Commun.* **2020**, *11*, 4037. [CrossRef]
23. Slobodeniuk, A.O.; Koperski, M.; Molas, M.R.; Kossacki, P.; Nogajewski, K.; Bartos, M.; Watanabe, K.; Taniguchi, T.; Faugeras, C.; Potemski, M. Fine structure of K-excitons in multilayers of transition metal dichalcogenides. *2D Mater.* **2019**, *6*, 025026. [CrossRef]
24. Niehues, I.; Blob, A.; Stiehm, T.; de Vasconcellos, S.M.; Bratschitsch, R. Interlayer excitons in bilayer MoS_2 under uniaxial tensile strain. *Nanoscale* **2019**, *11*, 12788–12792. [CrossRef] [PubMed]